Hierarchical crack pattern as formed by successive domain divisions. II. From disordered to deterministic behavior

S. Bohn*
Laboratoire de Physique Statistique, École Normale Supérieure, 24 Rue Lhomond, 75231 Paris Cedex 05, France and Magnasco Lab, The Rockefeller University, Box 212, 1230 York Avenue, New York, New York 10021, USA

J. Platkiewicz, B. Andreotti, M. Adda-Bedia, and Y. Couder
Laboratoire de Physique Statistique, École Normale Supérieure, 24 Rue Lhomond, 75231 Paris Cedex 05, France
(Received 8 December 2004; published 28 April 2005)

Hierarchical crack patterns, such as those formed in the glaze of ceramics or in desiccated layers of mud or gel, can be understood as a successive division of two-dimensional domains. We present an experimental study of the division of a single rectangular domain in drying starch and show that the dividing fracture essentially depends on the domain size, rescaled by the thickness of the cracking layer e. Utilizing basic assumptions regarding the conditions of crack nucleation, we show that the experimental results can be directly inferred from the equations of linear elasticity. Finally, we discuss the impact of these results on hierarchical crack patterns, and in particular the existence of a transition from disordered cracks at large scales—the first ones—to a deterministic behavior at small scales—the last cracks.

DOI: 10.1103/PhysRevE.71.046215 PACS number(s): 89.75.Kd, 46.50.+a, 47.54.+r

I. INTRODUCTION

Macroscopic patterns often present an intriguing interplay between a well-defined local organization and a globally disordered appearance. For instance, the geometry of two-dimensional soap foams [1] is perfectly defined locally: the films are arcs of circles joining at 120° in threefold vertices. Nevertheless, due to the distribution of bubble sizes and to their time evolution, the coarsening, the foam presents a disordered aspect at large scale, which has been intensively studied in recent decades [2]. While in this case, the apparent disorder results from a deterministic evolution, other systems are strongly influenced by uncontrolled experimental noise. The liquid flow in the case of viscous fingering is well described in the deterministic framework of fluid dynamics, but the sensitivity of the system close to bifurcation points makes the concrete evolution unpredictable: two experimental realizations never give identical results although the patterns are similar from the statistical point of view.

In the present paper, we study the interplay between deterministic behavior and the effect of noncharacterized noise in a particular system: hierarchical crack patterns. This kind of pattern can be found in the glaze of ceramics (Fig. 1) or—experimentally more accessible—in layers of mud or gel, deposited on a solid substrate and desiccating. The fractures are formed via mechanical frustration: the shrinking, induced either by cooling in the case of the glaze or by evaporation of the solvent in the case of the mud, is restricted by the adhesion to the rigid substrate. If the material layer is not too thin and sufficiently homogeneous, these cracks are formed successively [3,4]: one fracture has finished its propagation before the next one nucleates. The shape of a fracture is entirely determined by its path while it is propagating. A new fracture has no influence on the shape of the previous ones. However, these previous fractures having modified the mechanical stress field have a direct influence on the morphology of newer fractures. This asymmetrical interaction becomes manifest at the connection points. A fracture always propagates to release the main opening stress (principle of local symmetry). The stress parallel to a given crack is only weakly affected by its formation, so that, in the vicinity of an existing crack, the residual stresses are parallel to it. Therefore, when a new fracture comes near an older one, it turns to join it at a right angle. As discussed in paper I [18], it is possible, using these characteristics, to reconstruct the order of formation of the cracks of a complex pattern.

In one-dimensional systems, the correlation between successive cracks has been studied experimentally and theoretically. The study of a spring chain model coupled to a solid substrate [5] has revealed the existence of a characteristic length scale, which is a function of the spring constants and lengths. The identification with material properties and geometry is nevertheless not evident. The spacing between successive fractures along a line of desiccating clay with a rectangular cross section [6] could be interpreted as the

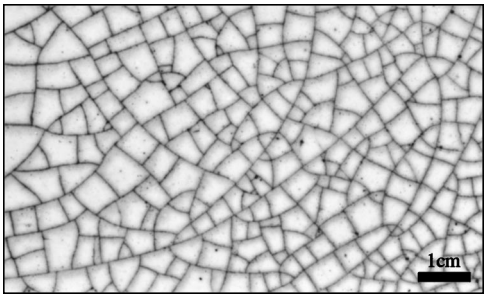

FIG. 1. The hierarchical crack pattern in the glaze of a ceramic plate.

*Electronic address: bohns@rockefeller.edu

experimental confirmation of this characteristic length. However, the size of the sample was kept fixed in [6] so that the physical origin of the length scale was not clear.

We will investigate here, in the two-dimensional case, the effect of previous fractures on the following ones. The basic feature on which this investigation relies is that each new fracture joins existing fractures at both ends, so that at each step of its formation the pattern divides space. Taking into account the succession of cracks, we can interpret the pattern as the result of an iterative process: a fracture divides a "mother" domain into two "daughter" domains [7], which can be considered—at least in the limit of a perfect rigid substrate—as mechanically independent. We can therefore consider each domain separately. From this perspective, the formation of the crack pattern is conceptually very simple: we need only to understand how *one* single domain is divided as a function of its shape and then take into account the inheritance of the domain shape from the former divisions.

The conceptual simplicity of the hierarchical crack pattern will allow us to study the interplay between a deterministic part—the control of fractures by the shape of the considered domain—and a stochastic part—the impact of uncontrolled imperfections of the material. For this purpose, we will investigate the division of a domain whose geometry is controlled. By contrast to the domains in an extended pattern whose shape is inherited from former divisions, this will allow a systematic study under reproducible conditions. We will successively present the experimental results, their interpretation in the framework of linear elasticity, and their consequences for extended crack patterns.

II. EXPERIMENT

In what follows, we study fractures in a desiccating starch-water mixture. While drying, the material shrinks, but due to the adhesion on a polymethylmethacrylate (PMMA) substrate, the shrinking is partly inhibited. The resulting stress is then released by the formation of fractures. We control the initial domain by lateral walls. The lateral dimension of the domains is fixed and we vary the layer thickness.

A. Set up and protocol

Figure 2(a) shows the container used, composed by a PMMA bottom and removable metallic walls. The inner dimensions of the metallic frame are 55×77.3 mm^2, its aspect ratio is thus $\sqrt{2}$. Before each experiment, the components are cleaned separately with a dishwasher solution and then rinsed carefully. The lateral walls are then coated with a very thin layer of silicone oil.

We mix maize starch with water in the relation of 1 to 1.15 g. The homogeneous solution is filled into the container. In order to obtain reproducible drying conditions and to accelerate the drying, the container is placed in a gently ventilated oven with a controlled temperature of 40 °C. When the starch is completely desiccated, a photograph of the crack pattern is taken.

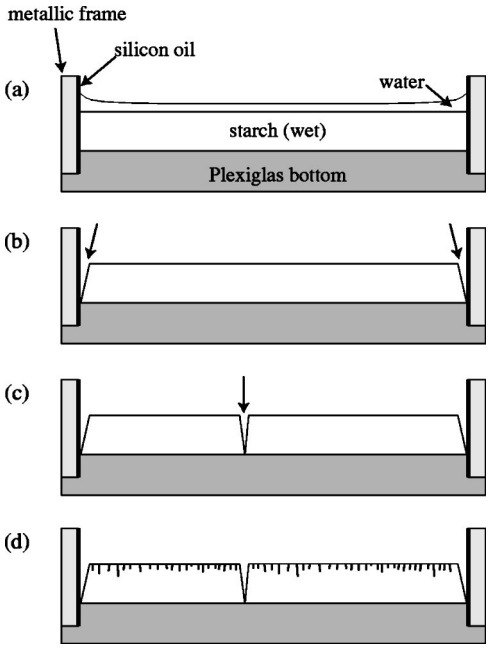

FIG. 2. Setup and evolution of the experiment. (a) Side view of the experiment. The starch solution is filled into the rectangular container with its lateral walls silicone oil coated. A water layer forms on the layer of wet starch. It evaporates and the starch layer becomes exposed to the air. (b) Due to the ongoing evaporation, the starch contracts and loses the contact to the lateral walls (arrows). (c) The first kind of fracture, called hierarchical, is formed (arrow). (d) The second cracking regime with small scale cracks penetrating simultaneously from the upper surface into the volume.

B. General behavior

In order to observe the temporal evolution of the system, we conduct some experiments outside the oven, place the container on a computer-controlled balance, and acquire a film. Figure 2 shows a sketch of the evolution; Fig. 3 some photographs of the system. First, the initially homogeneous solution separates into two phases [Fig. 2(a)]. A concentrated starch phase sediments to the bottom while water segregates on the top. Approximately half an hour after filling in the mixture, a thin and clear water layer is found on top of the

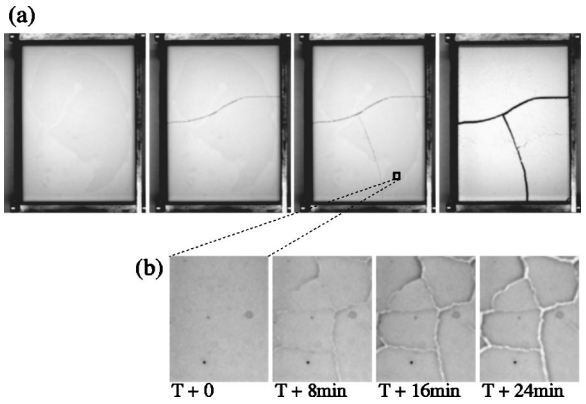

FIG. 3. Evolution of the system while drying. (a) The formation of hierarchical cracks. (b) Small, columnar cracking.

layer of wet starch. The surface of the water layer is curved at the border, due to the wetting on the oil-coated walls, but the starch layer remains perfectly planar. Actually, the initial mixture concentration was chosen to obtain this thin water layer that allows the bypassing lateral wetting problems.

It takes about eight hours to evaporate the water layer. The mass of the system decreases linearly (data not shown). Then, the wet starch layer is exposed to air and starts drying. The mass decrease is still linear in time, but slightly slower. The water evaporation induces a shrinkage of the material that is frustrated by the adhesion to the PMMA bottom, and—at the beginning—on the lateral walls. After another hour, the resulting mechanical tensions are sufficiently strong and a first kind of fracture appears: the starch layer gets separated from the oil-coated lateral walls [Fig. 2(b)]. The rectangular domain is now laterally delimited by free surfaces, just like domains in extended crack patterns. By contrast to the latter, the domain geometry is controlled by the shape of the container.

About one hour later, we observe the fracture of this controlled domain [Fig. 2(c)]. Figure 3(a) shows an example where two fractures are formed successively, so that the rectangular domain is ultimately divided into three subdomains. In general, these fractures, although successive, are formed in a relatively short time interval of half an hour. The fractures are nucleated on the upper surface of the starch layer somewhere close to the center of the domain. Though nucleated at the upper surface they quasi immediately affect the whole thickness of the layer. In the following hours, only the crack opening increases slowly and we do not observe any change in the evaporation rate.

Another, additional phenomenon is observed much later. After another seven hours of drying, a multitude of small and corrugated cracks appear simultaneously on the air-exposed surface [Figs. 2(d) and 3(b)]. The evaporation rate decreases continuously while these cracks are propagating downward into the bulk of the starch. As they penetrate, they become more ordered and show polygonal pattern as they reach the PMMA bottom. One observes a majority of hexagonal domains. This regime has been recently studied in [8–10]. If the experiment is performed in a container entirely made of polytetrafluoroethylene (Teflon) to prevent adhesion, no hierarchical cracking is observed but only the columnar cracking. This demonstrates that this latter phenomenon is not linked to the adhesion on the substrate. Rather we have here a three-dimensional (3D) directional fracturing, which follows a front of drying parallel to the surface and propagating downwards. The characteristic length scale of this hexagonal pattern ($\sim$3 mm) is much smaller than that of hierarchical fractures and scales probably with the depth over which the water content varies. They are analogs to the columnar cracking of basalt whose length scale is of the order of 1 m—the typical depth of the thermal boundary layer. In what follows, we focus on the first cracking regime, wherein hierarchical fractures form, due to the adhesion to the PMMA substrate.

C. Characteristic length scale of the final pattern

Figure 4 shows examples of the obtained hierarchical crack figures for different layer thicknesses e. A first and obvious observation is that the number of fractures increases when the layer thickness is decreased. For $e=6.3$ mm, there is only one fracture. In one of the examples shown [part 1 of Fig. 4(a)], the fracture does not reach the domain borders. Note also that, in some realizations at this thickness, no fracture was observed at all. Increasing the layer thickness, the number of realizations without fracture increases, and at $e=12$ mm, we never observed any fracture. We thus estimate the critical layer thickness for fractures roughly to $e\sim 10$ mm.

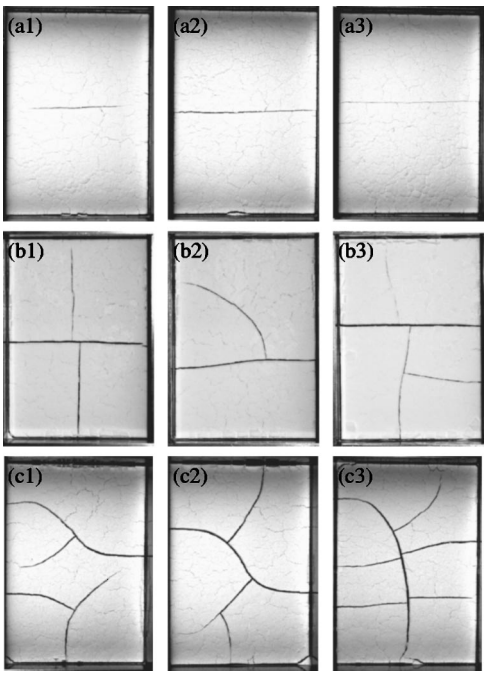

FIG. 4. Examples of crack patterns for different layer thicknesses. e= (a) 9.1, (b) 6.3, and (c) 4.8 mm.

In [3,4] it has been shown that the characteristic distance between the fractures scales linearly with the layer thickness. Although our experiment is not designed for this purpose, we observe qualitatively a similar behavior. We define the characteristic distance between cracks as

$$l=\sqrt{\frac{A}{N}} \tag{1}$$

where A is the area of the initial rectangular domain and N the number of domains in the final pattern. The length scale of the initial rectangle is $\sqrt{A}=65$ mm. Figure 5 shows this length as a function of the layer thickness e. Despite the dispersion, essentially due to the discrete—and small—number of cracks, the measurements suggest a linear relationship $l=\gamma e$. The best fit gives a slope $\gamma\sim 5.5$, consistent with the absence of fracture above $e=12$ mm.

D. The geometry of the first fracture

We will now concentrate on the first fracture that divides the rectangular domain into two daughter domains. Figure 4(a) shows three examples with a layer thickness $e=9.1$ mm. In all the three cases, the first (and only) fracture

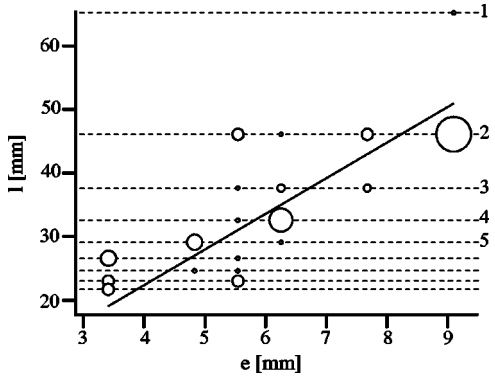

FIG. 5. The characteristic length scale of the domains in the final crack pattern $l=\sqrt{A/N}$ as a function of the layer thickness e. The small number N of domains (indicated on the right) leads to a very rough discretization. We indicated the number of realizations corresponding to a value by the radius of the symbol.

divides the rectangular domain symmetrically by the longer sides into two almost identical domains. In that case, the particular aspect ratio $\sqrt{2}$ of the initial domain is preserved in the division. We extract the first fracture using an image processing tool and superimpose all realizations at this layer thickness in Fig. 6(a). This fracture is perfectly reproducible. It is entirely determined by the free lateral boundaries. We observe furthermore that we are close to the limit of cracking: in two of ten realizations no fracture was observed at all.

The three examples in Fig. 4(b) are obtained for $e=6.3$ mm. The first fracture is still straight and perpendicular to the longer side of the rectangle. However, its position is less controlled, the fracture does not always pass by the center. Note also that the position of the first fracture has an impact on those that follow. The superposition of the first fracture of all experiments at this layer thickness is shown in Fig. 6(b). Only in one case did the fracture turn to join one of the shorter borders of the sample, probably because of a defective preparation of the sample. As can be seen in Fig. 6(c), the loss of determinism increases when the layer thickness is decreased. The first fracture is now not only free to choose its position, but it also starts to bend significantly in some realizations.

This behavior becomes more and more dominant as the layer thickness is further decreased [Figs. 6(d) and 6(e)]. The fracture joins a short side of the rectangle at one or even both ends. It is less and less controlled by the domain shape. Only when it arrives relatively close to the border does the fracture turn to join it at right angle. As can be seen in the figures, even for small layer thicknesses such as $e=4.8$ or 3.4 mm [Figs. 6(d) and 6(e)], the first fracture sometimes is the same as the deterministic "ideal" one, observed for thicker layers close to the cracking limit.

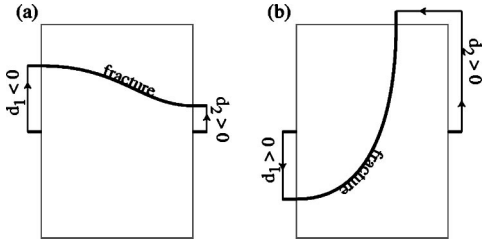

FIG. 7. Definition of the two distances d_1 and d_2.

A simple way to interpret this behavior is as follows: the "fractures" that define the border of the domain relax the mechanical stress locally. They have an impact only over a distance that is proportional to the layer thickness. In the center of a very large domain of small thickness, their influence vanishes. By contrast, in a small domain compared to the layer thickness, they have a direct impact over the whole domain area. This interpretation leads us to introduce dimensionless quantities.

E. Quantifying

In order to quantify the observed transition from determinism to disorder, we introduce two quantities—two order parameters—that are consistent with the symmetries of the geometry. Let us first define the distances d_1 and d_2 of the end of the fracture to the center of the long side of the rectangle, measured along the domain perimeter (see geometrical definition in Fig. 7). It can be positive or negative if the crack extremity is on the right or left side of the center. We define the two dimensionless order parameters as

$$\delta = |d_1 + d_2|/\sqrt{A}, \tag{2}$$

$$\Delta = \sqrt{d_1^2 + d_2^2}/\sqrt{A}. \tag{3}$$

Their geometrical meaning is as follows. In the case of the ideal fracture that passes through the center and divides the rectangular domain into two symmetric rectangular domains, both δ and Δ are equal to zero. If the fracture is still straight and perpendicular to the longer sides of the rectangle but does not pass by the center, $\delta=0$ but $\Delta>0$. When the fracture is curved, δ becomes larger than zero, too. Figure 8 shows the scatter plot of these quantities as a function of the dimensionless layer thickness

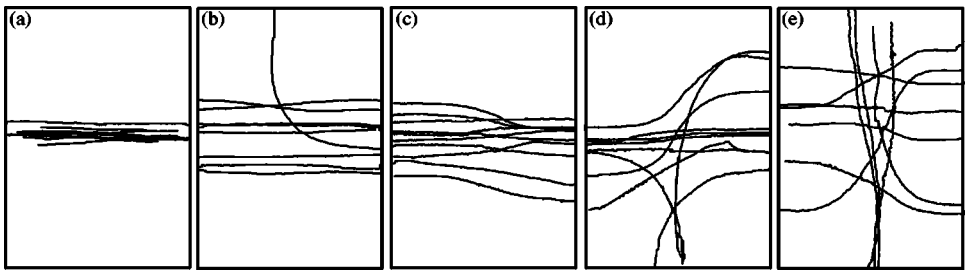

FIG. 6. The superposition of the first crack in several realizations. e= (a) 9.1, (b) 6.3, (c) 5.5, (d) 4.8, and (e) 3.4 mm.

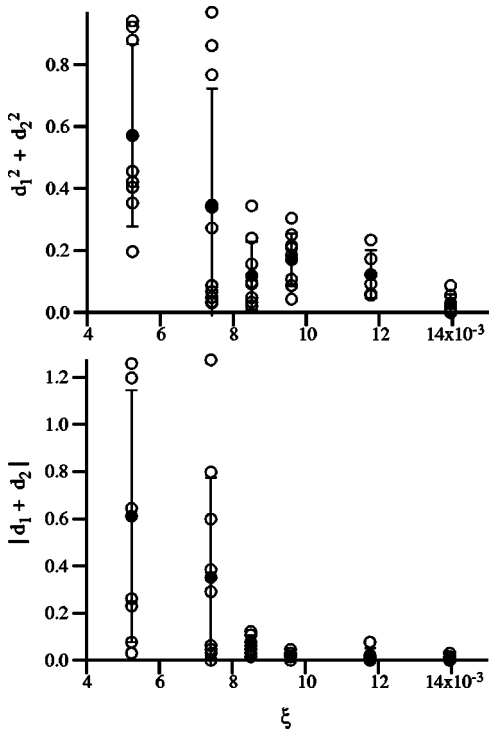

FIG. 8. The two order parameters $\delta=|d_1+d_2|/\sqrt{A}$ and $\Delta=\sqrt{d_1^2+d_2^2}/\sqrt{A}$ as functions of the ratio between the layer thickness and the characteristic domain size $\xi=e/\sqrt{A}$.

$$\xi = e/\sqrt{A}. \tag{4}$$

The filled symbols correspond to the averaged values and the error bars to the standard deviation. These two graphs summarize the discussed behavior. The cracking limit corresponds to $\xi\sim 0.18$ (11.2 mm for our experiment) so that there are no data points above this value. Close to this limit, $0.13\lesssim\xi\lesssim 0.18$, $\delta=0$ and $\Delta=0$. The fracture is the ideal, deterministic one. For $\xi\lesssim 0.13$, the fracture becomes statistically free to move laterally ($\Delta>0$), and this freedoom increases with decreasing ξ. The curving (δ) of the fractures sets in later, at straight fracture $\xi\lesssim 0.09$ and increases rapidly for decreasing ξ.

III. THEORY

Crack nucleation in this experiment can be influenced by two sources of randomness. First, it may be seen as a thermally activated process whose energy barrier decreases with the stress and even vanishes at a critical stress. Second, the stress field is itself affected by the existence of uncontrolled defects. Alternatively, we can consider the mean stress field that sets in the material due to the drying process and assume that the critical stress above which cracks nucleate has some random spatial noise. For simplicity, we perform an elastostatic analysis in the framework of two-dimensional linear elasticity. The configuration of the model problem analyzed is depicted in Fig. 9. A rectangular body of length L and height e perfectly adheres to a rigid substrate and sustains a shrinkage process induced by drying. We choose the height of the sample e as a unit length and define

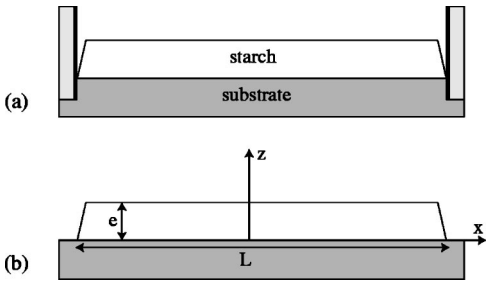

FIG. 9. The two-dimensional problem: the starch layer on the solid substrate. (a) Side view of the experiment. (b) The geometry used for the calculations.

$$\xi = \frac{2e}{L},$$

as the relevant control parameter of the problem. We scale the stress and strain tensor in such a way that under plane strain conditions, the two-dimensional strain tensor $\bar{\bar{\epsilon}}$ is related to the two-dimensional stress tensor $\bar{\bar{\sigma}}$ by

$$\sigma_{ij} = (1-2\nu)\epsilon_{ij} + \nu\epsilon_{kk}\delta_{ij} + \gamma\delta_{ij}, \tag{5}$$

where ν is the Poisson ratio of the sample. The plane stress in a two-dimensional description is simply obtained by replacing in Eq. (5) the Poisson ratio ν by $\nu/(1+\nu)$. The drying induced shrinkage of the material is taken into account by the diagonal term $\gamma\delta_{ij}$ in Eq. (5). In the case of free boundaries, the stress field in the sample would be identically zero and the strain field is simply given by $\epsilon_{ij}=-\gamma\delta_{ij}$. In the present description, we are interested in the spatial distribution of the stress and strain fields and not in their absolute magnitudes. Therefore, we can rescale stress and strain fields so that $\gamma=1$. The mechanical equilibrium in the material is given by

$$(1-2\nu)\Delta\vec{u} + \vec{\nabla}\cdot(\vec{\nabla}\cdot\vec{u}) = 0, \tag{6}$$

where $\vec{u}$ is the displacement field, which is related to the strain field by

$$\epsilon_{ij} = \frac{1}{2}\left[\frac{\partial u_i}{\partial x_j} + \frac{\partial u_j}{\partial x_i}\right].$$

The boundary conditions at the lower surface $z=0$ are specified by assuming a perfect adhesion of the sample to the rigid substrate. The upper and lateral surfaces ($z=1$ and $x=\pm 1/\xi$) are traction free. The boundary conditions for this problem are thus given by

$$u_x(x,0) = u_z(x,0) = 0, \tag{7}$$

$$\sigma_{xz}(x,1) = \sigma_{zz}(x,1) = 0, \tag{8}$$

$$\sigma_{xz}(\pm 1/\xi, z) = \sigma_{xx}(\pm 1/\xi, z) = 0. \tag{9}$$

At this stage, the problem depends only on the Poisson ratio ν and on the dimensionless parameter ξ. Experimentally, we observe that fractures are nucleated on the upper free surface of the material ($z=1$). Therefore, the quantity of interest in the present problem is $\sigma_{xx}(x,1)$, the stress distribution there.

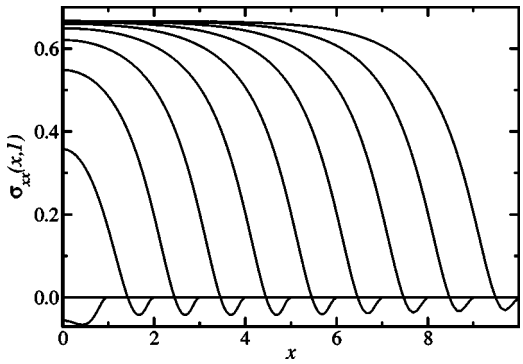

FIG. 10. Plot of $\sigma_{xx}(x,1)$ for $\nu=0.25$ and for different values of ξ. Due to the symmetry with respect to $x=0$, only the interval $0<x<\xi^{-1}$ is shown. The values of ξ are from left to right such that $\xi^{-1}=1$, 2, 3, 4, 5, 6, 7, 8, 9, and 10.

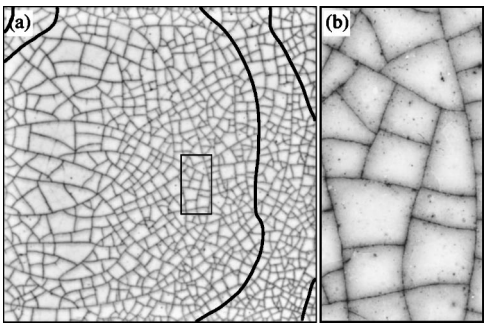

FIG. 11. A crack pattern in the glaze of an ceramic plate. (a) The entire plate (size 14.5×14.5 cm^2). The first order cracks are emphasized manually. (b) The detail of the pattern indicated by the frame in (a).

An analytical solution to the present problem with a finite thickness is unreachable. However, the asymptotic value for the stress in very thin layers, far from the lateral boundaries, can be easily computed. In the absence of the lateral boundaries ($\xi\to0$), the stress and strain fields are uniform throughout the thickness and the only nonvanishing components are σ_{xx} and ϵ_{zz}. Using Eq. (5), one finds

$$\lim_{\xi\to0}\sigma_{xx}(x,1)=\frac{1-2\nu}{1-\nu}. \tag{10}$$

For a finite rectangular plate, the numerical resolution of the problem is straightforward. We use a standard finite element formulation and solve it for each value of the parameters ν and ξ.

Figure 10 summarizes the numerical results of this section. The stress component on the upper free surface of the material, $\sigma_{xx}(x,1)$, is plotted for different values of ξ and for a given Poisson ratio ($\nu=0.25$). It is shown that when the height of the sample is comparable to its length (ξ of order unity), the tensile stress at the center of the sample is compressive ($\sigma_{xx}(0,1)<0$), which does not allow crack nucleation in that region. When ξ decreases, which corresponds to a thinner sample, the stress shows a positive maximum at the center $x=0$, which allows us to predict that there will be a critical value ξ for the nucleation of a crack which is localized at the center $x=0$. However, when one decreases further ξ, the maximum in the medium of the plate becomes less manifest and tends to the value given by Eq. (10). In a large region around the center the variation of the tensile stress becomes weaker and thus, due to the inherent inhomogeneities induced by noise, the nucleation of the fracture will not be localized at $x=0$. This simple description of the drying induced shrinkage shows the importance of the aspect ratio e/L on the stress distribution in the material and thus explains the phenomenon observed in experiments.

IV. CONCLUSION

The experimental results presented here, together with the theoretical considerations, provide a coherent image of the relative impact of the domain shape on the cracks that divide it. The domain borders—the older cracks—relax the stress locally. Their influence is determined by the characteristic length scale, the layer thickness e. Far away from the borders, they do not affect the stress field and thus the crack formation. The zone of crack nucleation (in a probabilistic sense) inside a given domain has thus roughly the same shape as the domain albeit shifted by several thicknesses e.

We argued in the first paper that we can consider an extended crack pattern as resulting from successive domain divisions. The results presented in the present part indicate the effect the shape of a mother domain has on the fracture that divides it. Let us consider the pattern in Fig. 11. As we go down the hierarchy, the length of the cracks and the size A of the domains decrease. As the thickness remains constant, the dimensionless parameter $\xi=e/\sqrt{A}$ increases during the successive divisions. For the first cracks, the domain size is much larger than the layer thickness, and the cracks are mostly dominated by the imperfections of the layer (global gradients, defects). They thus have a disordered appearance. Moreover, when a crack nucleates on a defect, or simply passes through it, the latter disappears and has no impact on the following fractures. The spatial random noise level thus decreases with the passing of time. As cracks keep dividing the domains their typical size decreases until it becomes comparable to the layer thickness. Here, the cracks becomes deterministic and are entirely controlled by the domain borders [Fig. 11(b)].

This transition from disorder at large scales to determinism at small scales contrasts with a scaling behavior that is repeatedly found in numerical and experimental studies of nonhierarchical cracking [11–15] and also experimentally for the fracture widths in hierarchical crack patterns [16,17]. The existence of a characteristic length scale, the layer thickness e, is the reason why we do *not* observe self-similar behavior for the domain shapes and crack-crack interaction. This is consistent with the fact that there is a well-defined characteristic domain size in the final pattern, which scales with the layer thickness [3,4]. The larger variations of the domain size in Fig. 11(a) are due to a global thickness gradient; the domain size distribution is only slightly disperse. The considered successive domain divisions are therefore an illustrative example that not everything in nature is fractal.

[1] D. Weaire and S. Hutzler, *The Physics of Foams* (Clarendon Press, Oxford/Oxford University Press, New York, 1999).
[2] J. Stavans, Rep. Prog. Phys. **56**, 733 (1993).
[3] A. Groisman and E. Kaplan, Europhys. Lett. **25**, 415 (1994).
[4] K. Shorlin, J. de Bruyn, M. Graham, and S. Morris, Phys. Rev. E **61**, 6950 (2000).
[5] O. Morgenstern, I. Sokolov, and A. Blumen, J. Phys. A **26**, 4521 (1993).
[6] N. Lecocq and N. Vandewalle, Eur. Phys. J. E **8**, 445 (2002).
[7] S. Bohn, S. Douady, and Y. Couder, Phys. Rev. Lett. **94**, 054503 (2005).
[8] G. Müller, J. Struct. Geol. **23**, 45 (2001).
[9] L. Goehring and S. W. Morris, Europhys. Lett. **69**, 739 (2005).
[10] E. A. Jagla and A. G. Rojo, Phys. Rev. E **65**, 026203 (2002).
[11] S. Kitsunezaki, Phys. Rev. E **60**, 6449 (1999).
[12] L. de Arcangelis and H. Herrmann, Phys. Rev. B **39**, 2678 (1989).
[13] H. Colina, L. de Arcangelis, and S. Roux, Phys. Rev. B **48**, 3666 (1993).
[14] T. Walmann, A. Malthe-Sorenssen, J. Feder, T. Jssang, P. Meakin, and H. Hardy, Phys. Rev. Lett. **77**, 5393 (1996).
[15] R. Cafiero, G. Caldarelli, and A. Gabrielli, J. Phys. A **33**, 8013 (2000).
[16] D. Mal, S. Sinha, S. Mitra, and S. Tarafdar, Physica A **346**, 110 (2004).
[17] N. Lecocq and N. Vandewalle, Physica A **321**, 431 (2003).
[18] S. Bohn, L. Pauchard, and Y. Couder, preceding paper, Phys. Rev. E **71**, 046214 (2005).